

Transport properties of highly conductive *n*-type Al-rich Al_xGa_{1-x}N ($x \geq 0.7$)

M. L. Nakarmi, K. H. Kim, K. Zhu, J. Y. Lin, and H. X. Jiang^{a)}
Department of Physics, Kansas State University, Manhattan, Kansas 66506-2601

(Received 5 February 2004; accepted 2 September 2004)

We report here the growth and transport studies of conductive *n*-type Al_xGa_{1-x}N alloys with high Al contents ($x \geq 0.7$). Si-doped Al_xGa_{1-x}N alloys were grown by metalorganic chemical vapor deposition on AlN-epilayer/sapphire substrates with very smooth surface. Low *n*-type resistivities have been obtained for Al-rich Al_xGa_{1-x}N alloys. The resistivity was observed to increase rapidly with increasing x due to the deepening of the Si donor energy level. Transport measurements have indicated that we have achieved *n*-type conduction in pure AlN. From the temperature dependence of the resistivity, the donor activation energy was estimated to vary from 23 to 180 meV as x was increased from 0.7 to 1.0. © 2004 American Institute of Physics.
 [DOI: 10.1063/1.1809272]

Al-rich AlGa_N alloys, covering wavelengths from 300 to 200 nm, are ideal materials for the development of chip-scale UV light sources/sensors, because AlGa_N is the ultrawide band-gap semiconductor system in which the band gap can be easily engineered through the use of alloying and heterostructure design. Efficient solid-state UV light sources/sensors are crucial in many fields of research and development. For instance, protein fluorescence is generally excited by UV light; monitoring changes of intrinsic fluorescence in a protein can provide important information on its structural changes.¹ Thus, the availability of chip-scale UV light sources is expected to open up new opportunities for medical research and health care. Solid-state UV light sources also have applications in water purification, equipment/personnel decontamination, and white light generation.² Recently, several groups have successfully demonstrated the operation of deep UV emitters based on AlGa_N alloys.³⁻⁶ However, achieving highly conductive *n*-type and *p*-type Al_xGa_{1-x}N alloys with high Al contents ($x > 0.6$) is essential for the realization of high performance practical devices.

We have previously reported the results for *n*-type conductive Al_xGa_{1-x}N alloys for x up to 0.7; a resistivity value of 0.15 Ω cm (with a free electron concentration of $2.1 \times 10^{18} \text{ cm}^{-3}$ and mobility of 20 cm²/V s) was achieved for Al_{0.65}Ga_{0.35}N.^{7,8} Recently, using In-Si co-doping, *n*-type Al_{0.65}Ga_{0.35}N has been obtained with an electron concentration of $2.5 \times 10^{19} \text{ cm}^{-3}$ and mobility of 22 cm²/V s, corresponding to a resistivity of 0.011 Ω cm.⁹ There were also several studies on Si doped AlN.^{10,11} An electron concentration of $9.5 \times 10^{16} \text{ cm}^{-3}$ in Si doped AlN was obtained; however, no resistivity value was reported.¹⁰

In this letter, we report on the epitaxial growth and transport studies of Si-doped *n*-type Al-rich Al_xGa_{1-x}N epilayers ($x \geq 0.7$) with low resistivities. Al-rich Al_xGa_{1-x}N epilayers ($x \geq 0.7$) were grown on sapphire substrates by MOCVD with a thickness of about 1 μm. A 0.5 μm AlN epilayer was first deposited on (0001) sapphire substrate with a low temperature buffer, followed by the growth of Si-doped Al_xGa_{1-x}N epilayer. The targeted Si-dopant concentration (N_{Si}) was around $4 \times 10^{19} \text{ cm}^{-3}$ in all samples. The metalorganic sources used were trimethylgallium (TMGa) for Ga

and trimethylaluminum (TMAI) for Al, respectively. Blue ammonia and silane (SiH₄) were used as nitrogen and silicon sources, respectively. Variable temperature Hall-effect (Standard Van der Pauw) measurement was employed to measure the electron concentration, mobility and resistivity. X-ray diffraction and photoluminescence were used to determine the Al content and the crystalline quality of AlGa_N epilayers. Atomic force microscope (AFM) was used to study the surface morphology; no crack was found for all samples studied in this work.

Achieving highly conductive Al_xGa_{1-x}N alloys with high Al contents is known to be very challenging due to several well-known mechanisms: (i) an increase in the ionization energy of the dopants with increasing Al content¹² and (ii) the formation energy of Al vacancy (V_{Al}) decreases with increasing Al content and becomes very low with a triple negatively charged state in AlN (V_{Al}^{3-}).¹³⁻¹⁵ It is known that oxygen impurity incorporation as well as the presence of dislocations can enhance the formation of cation vacancies during the nitride crystal growth to form energetically stable V_{Al} or $V_{\text{Al}}\text{-O}_{\text{N}}$ complexes.¹³⁻¹⁷ We thus believe that high oxygen impurity and dislocation densities translate to a reduced conductivity in AlGa_N and AlN and that it is necessary to control the oxygen impurity and dislocation densities before *n*-type conductivity can be improved in AlGa_N with high Al contents. Figure 1 shows the oxygen and carbon impurity profiles as measured by SIMS for an AlN epilayer, indicating that the oxygen concentration in our epilayers is quite low ($\sim 2 \times 10^{17} \text{ cm}^{-3}$). This is one of the keys for achieving highly conductive Al-rich AlGa_N alloys. Furthermore, the use of high quality AlN-epilayer/sapphire as a template for the subsequent growth of Si-doped layers is also essential for attaining highly conductive Al-rich epilayers. The benefits of inserting AlN epitaxial layer as a template for dislocation density reduction have been demonstrated in several previous experiments.^{18,19}

Figure 2 presents the room temperature Hall measurement results of *n*-Al_xGa_{1-x}N ($x \geq 0.7$), showing the Al content (x) dependent resistivity (a), electron concentration (b), and electron mobility (c), respectively. Figure 2 shows that we have achieved low room temperature *n*-type resistivities for Al-rich AlGa_N alloys. For instant, a low resistivity of 0.0075 Ω cm (with an electron concentration of 3.3

^{a)}Electronic mail: jiang@phys.ksu.edu

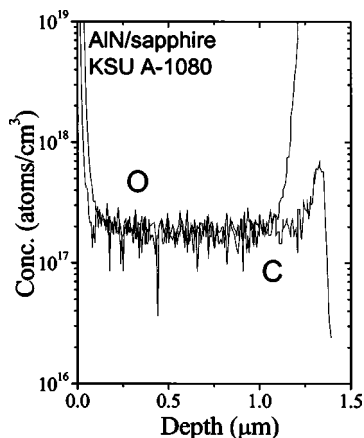


FIG. 1. Oxygen and carbon impurity profiles in an AlN epilayer, as probed by SIMS (performed by Charles Evans & Associate).

$\times 10^{19} \text{ cm}^{-3}$ and mobility of $25 \text{ cm}^2/\text{V s}$) has been obtained for $\text{Al}_{0.7}\text{Ga}_{0.3}\text{N}$. The measured resistivity increases with the Al content (x) very rapidly and the dependence can be described by the following empirical equation:

$$\rho(\text{Al}_x\text{Ga}_{1-x}\text{N}) = \rho(\text{AlN}) \times 10^{-(1-x)/0.08}, \quad (1)$$

from which one can deduce that the resistivity of $n\text{-Al}_x\text{Ga}_{1-x}\text{N}$ ($x > 0.7$) increases by about one order of magnitude when Al content (x) is increased by about 8%. This rapid increase in resistivity is predominantly due to the increase in donor ionization energy with x .

The temperature-dependent resistivity results for $n\text{-Al}_x\text{Ga}_{1-x}\text{N}$ ($x \geq 0.7$) in the temperature range from 70 to 650 K are shown in Fig. 3. Strong temperature dependence is observed, especially for samples with high Al content ($x > 0.8$). The Al content dependence of the donor activation energy E_0 can be estimated by fitting the temperature-dependent resistivity data with the following thermal activation behavior:

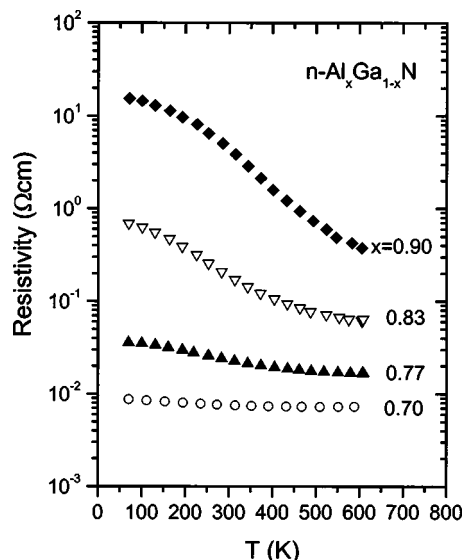


FIG. 3. Comparison of temperature-dependent resistivity results for $n\text{-Al}_x\text{Ga}_{1-x}\text{N}$ of different x ($x \geq 0.7$).

$$\rho = \rho_0 [1 + C \exp(-E_0/kT)], \quad (2)$$

where C is a fitting constant and k is the Boltzmann constant. The inset of Fig. 4 illustrates an example of this fitting process for $\text{Al}_{0.77}\text{Ga}_{0.23}\text{N}$, where a value of 41 meV for E_0 was obtained for this sample. The Al content dependence of E_0 is depicted in Fig. 4, which clearly shows that E_0 increases linearly with an increase of the Al content. This deepening of E_0 is due to the fact that with an increase of the Al content in AlGa_{1-x}N alloys, band gap and electron effective mass increase, while the dielectric constant and band gap renormalization effect decrease. An estimated value of about 180 meV for E_0 in pure AlN was obtained, which is larger than the value of about 85 meV obtained by Taniyasu *et al.*¹⁰ This discrepancy may be due to the fact that the donor activation energy varies with Si doping level due to the band gap renormalization effect.

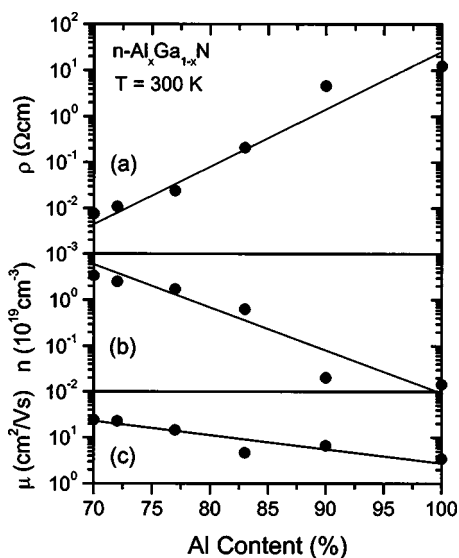


FIG. 2. Room temperature Hall measurement results of $n\text{-Al}_x\text{Ga}_{1-x}\text{N}$ ($x \geq 0.7$). (a), (b), and (c) The Al content (x) dependent resistivity, electron concentration, and electron mobility, respectively; lines are guides for the eye.

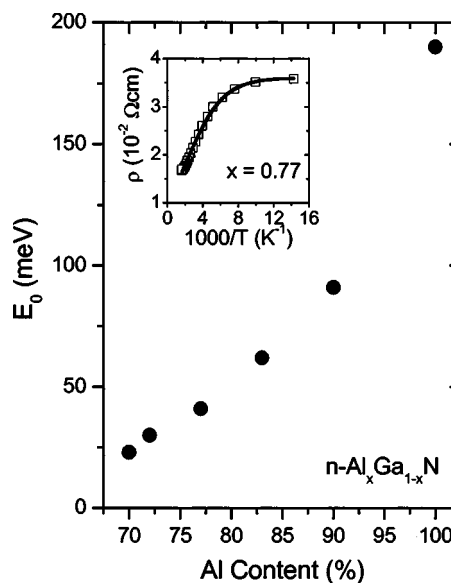


FIG. 4. Si donor activation energy as a function of the Al content, x , estimated from the temperature-dependent resistivity results. The inset shows the Arrhenius plot of the resistivity of $n\text{-Al}_{0.77}\text{Ga}_{0.23}\text{N}$ and an activation energy of 41 meV was obtained.

We believe that, for optimized materials, the predominant cause for the rapid increase in resistivity of $\text{Al}_x\text{Ga}_{1-x}\text{N}$ alloys with increasing x is the Si donor energy level deepening. To further illustrate this point, we have plotted the measured room temperature resistivity (ρ) as a function of Si donor activation energy (E_0) in a semi-logarithmic scale (not shown), which follows a linear behavior for larger E_0 values except the AlN data point. This behavior is a direct consequence of Eq. (2), which can be approximately written as $\rho \propto \exp(E_0)$ at a fixed temperature when $E_0 > kT$. Thus, the resistivity (ρ) of $\text{Al}_x\text{Ga}_{1-x}\text{N}$ alloys with high Al contents increases exponentially with the Si donor activation energy (E_0).

Our experimental results indicate that we have achieved measurable room temperature n -type conductivity in pure AlN. The effect of persistent photoconductivity has been observed in Si-doped AlN grown by MBE, suggesting that Si may undergo a DX-like metastability.²⁰ However, our experimental results presented here together with the previous study by Taniyasu *et al.* seem to suggest that silicon impurities act more like an effective mass state, in agreement with a previous theoretical prediction.¹⁵ These discrepancies may be accounted for by the fact that the concentrations of oxygen impurities and hence Al vacancies (or $V_{\text{Al}}\text{-O}_{\text{N}}$ complexes) have been significantly reduced in highly conductive AlGaN alloys studied here.

In summary, by controlling the oxygen impurity concentration, thereby minimizing the generation of Al vacancies, n -type $\text{Al}_x\text{Ga}_{1-x}\text{N}$ ($x \geq 0.7$) epilayers on AlN epilayer/sapphire substrates by MOCVD with low resistivities have been obtained. It was shown that silicon impurities act as shallow donors in all samples studied here. The donor activation energy E_0 was found to increase from 23 meV for $\text{Al}_{0.7}\text{Ga}_{0.3}\text{N}$ up to 180 meV for AlN. The increase in E_0 results in a rapid increase in resistivity, roughly by one order of magnitude for every 8% increase in Al content. By further optimizing the growth condition and hence minimizing the effects of impurity compensation, it is possible to further

improve the conductivity of pure AlN by heavy doping.

This research is supported by grants from NSF, DOE, ARO, and DARPA.

- ¹J. R. Lakowicz, *Principles of Fluorescence Spectroscopy*, 2nd ed. (Kluwer Academic, New York, 1999).
- ²A. Bergh, G. Craford, A. Duggal, and R. Haitz, *Phys. Today* **54**, 42 (2001).
- ³A. Chitnis, J. P. Zhang, V. Adivarahan, M. Shatalov, S. Wu, R. Pachipulusu, V. Mandavilli, and M. Asif Khan, *Appl. Phys. Lett.* **82**, 2565 (2003).
- ⁴J. P. Zhang, A. Chitnis, V. Adivarahan, S. Wu, V. Mandavilli, R. Pachipulusu, M. Shatalov, G. S. Simin, J. W. Yang, and M. Asif Khan, *Appl. Phys. Lett.* **81**, 4910 (2002).
- ⁵A. Yasan, R. McClintock, K. Mayes, D. Shiell, L. Gautero, S. R. Darwish, P. Kung, and M. Razeghi, *Appl. Phys. Lett.* **83**, 4701 (2003).
- ⁶K. H. Kim, J. Li, S. X. Jin, J. Y. Lin, and H. X. Jiang, *Appl. Phys. Lett.* **83**, 566 (2003).
- ⁷J. Li, K. B. Nam, J. Y. Lin, and H. X. Jiang, *Appl. Phys. Lett.* **79**, 3245 (2001).
- ⁸K. B. Nam, J. Li, M. L. Nakarmi, J. Y. Lin, and H. X. Jiang, *Appl. Phys. Lett.* **81**, 1038 (2002).
- ⁹P. Cantu, S. Keller, U. K. Mishra, and S. P. DenBaars, *Appl. Phys. Lett.* **82**, 3683 (2003).
- ¹⁰Y. Taniyasu, M. Kasu, and N. Kobayasu, *Appl. Phys. Lett.* **81**, 1255 (2002).
- ¹¹K. B. Nam, M. L. Nakarmi, J. Li, J. Y. Lin, and H. X. Jiang, *Appl. Phys. Lett.* **83**, 2787 (2003).
- ¹²B. Jahn, M. Albrecht, W. Dorsch, S. Christiansen, H. P. Strunck, D. Hanser, and R. F. Davis, *MRS Internet J. Nitride Semicond. Res.* **3**, 39 (1998).
- ¹³C. G. Van de Walle and J. Neugebauer, *J. Appl. Phys.* **95**, 3851 (2004).
- ¹⁴T. Mattila and R. M. Nieminen, *Phys. Rev. B* **55**, 9571 (1997).
- ¹⁵C. Stampfl and C. G. Van de Walle, *Appl. Phys. Lett.* **72**, 459 (1998).
- ¹⁶J. Oila, J. Kivioja, V. Ranki, K. Saarinen, D. C. Look, R. J. Molnar, S. S. Park, S. K. Lee, and J. Y. Han, *Appl. Phys. Lett.* **82**, 3433 (2003).
- ¹⁷J. Neugebauer and C. G. Van de Walle, *Appl. Phys. Lett.* **69**, 503 (1996).
- ¹⁸S. Arulkumaran, M. Sakai, T. Egawa, H. Ishikawa, T. Jimbo, T. Shibata, K. Asai, S. Sumiya, Y. Kuraoka, M. Tanaka, and O. Oda, *Appl. Phys. Lett.* **81**, 1131 (2002).
- ¹⁹B. Zhang, T. Egawa, H. Ishikawa, Y. Liu, and T. Jimbo, *J. Appl. Phys.* **95**, 3170 (2004).
- ²⁰R. Zeisel, M. W. Bayerl, S. T. B. Goennenwein, R. Dimitrov, O. Ambacher, M. S. Brandt, and M. Stutzmann, *Phys. Rev. B* **61**, R16283 (2000).